International Immunology, Vol. 21, No. 11, pp. 1225–1237
doi:10.1093/intimm/dxp090

Enhanced B cell activation in the absence of CD81

Mrinmoy Sanyal, Rosemary Fernandez and **Shoshana Levy**

Division of Oncology, Department of Medicine, Stanford University School of Medicine, Stanford, CA 94305, USA

Keywords: B cell activation, calcium mobilization, knockout, signal transduction, tetraspanin, TLR4

Abstract

CD81 is a component of the CD19/CD21 co-receptor complex in B cells. However, the role of CD81 in B cell activation has not been clearly elucidated. Here, we demonstrate that *Cd81*$^{-/-}$ B cells stimulated via their B cell receptor fluxed higher intracellular-free calcium ion along with increased phosphorylation of spleen tyrosine kinase and phospholipase gamma 2. Additionally, *Cd81*$^{-/-}$ B cells responded to toll like receptor 4 stimulation with increased nuclear factor-kappa B activation, cell proliferation and antibody secretion compared with wild-type B cells. *Cd81*$^{-/-}$ mice also mounted a significantly higher immune response to T-independent antigens than their wild-type counterparts. Finally, analysis of *Cd81*$^{-/-}$ B cells that were generated by bone marrow transplantation into *Rag1*$^{-/-}$ mice confirmed that the hyperactive phenotype is not dependent on the CD81-deficient environment. Taken together, these results indicate that CD81 plays a negative role in B cell activation *in vitro* and *in vivo*.

Introduction

CD81 is a tetraspanin molecule—it is embedded in the plasma membrane by four transmembrane domains that flank a small and a large extracellular loop and short amino and carboxyl termini (1). Most eukaryotic species, including fungi, plants, insects and vertebrates, express members of this family, implying that tetraspanins play an important physiological role (2, 3). Tetraspanins tend to associate with partner proteins and with each other in subcellular tetraspanin-enriched microdomains (TEMs), which are dynamic membrane entities that serve as signaling platforms (2, 3). The composition of individual TEMs within a single cell varies (4). Thus, the complexity of their interactions with each other and with partner proteins makes it difficult to decipher the independent function of tetraspanins.

The tetraspanin CD81 is widely expressed and is associated with different partner proteins in different cell lineages (5). CD81 has been implicated in diverse biological interactions, including egg-sperm and muscle cell fusion, syncytium formation and in immune and viral synapses (2, 3). Importantly, two major human pathogens, hepatitis C virus (6) and the malaria causing *Plasmodium falciparum* (7), depend on CD81 for at least one step of their infection cycle.

In B lymphocytes, CD81 associates directly with CD19 and indirectly with CD21 (8, 9). Co-engagement of the B cell receptor (BCR) and the CD19/CD21/CD81 co-receptor complex has been shown to reduce the threshold of B cell activation (10). This is a recognition mechanism that bridges the innate and adaptive immune systems, where opsonized antigens bind BCR and the complement receptor (CD21) and dually activate signal transduction via $Ig_{\alpha/\beta}$ and via the signaling molecule CD19 (11–15).

CD81 is required for normal cell surface expression of CD19. Genetic ablation of CD81 in three independently derived lines of mice led to a consistent reduction in CD19 expression (16–18). In addition, a CD81-deficient patient was recently identified who lacked CD19 expression in her B cells (19). Thus, normal expression of CD19 both in mice and in human is dependent on CD81. Moreover, in mice, this reduction of CD19 expression can be corrected by re-expression of human CD81 *in vivo* and *in vitro* (20–22).

Despite the consistent finding that CD19 expression is reduced in the absence of CD81, a clear role for CD81 in B cell function has not emerged (16–18). *In vitro* analyses of the B cell response to BCR stimulation have not given consistent results (17, 18). Similarly, inconsistent results have been obtained from *in vivo* immunization studies of the different CD81-deficient lines (16–18). Therefore, we re-examined the role of CD81 in B cell function. We show by various measures that activation of *Cd81*$^{-/-}$ B cells *in vitro* either through the BCR or through the toll like receptor (TLR) 4 pathway resulted in a hyperactive cellular response. In addition, *Cd81*$^{-/-}$ mice mounted increased immune responses to T-independent antigens *in vivo*. These observations are consistent with each other and suggest that CD81 functions as a negative regulator of B cell activation.

Correspondence to: S. Levy; E-mail: slevy@stanford.edu

Received 16 January 2009, *accepted* 6 August 2009

Transmitting editor: P. W. Kincade

Advance Access publication 7 September 2009

Methods

Mice

Heterozygous mice from the eighth backcross to BALB/c were bred and *Cd81*$^{-/-}$ and wild-type littermates were used in these studies (16). These and BALB/c *Rag1*$^{-/-}$ mice were bred at Stanford. All animals were maintained at Stanford according to Public Health Service Policy for Humane Care and Use of Laboratory Animals.

Antibodies

The following antibodies were conjugated with fluorochrome at Stanford University: M1/70 (anti-Mac-1/CD11b), 8C5 (anti-Gr-1), 6B2 (anti-B220), 145-2C11 (anti-CD3), GK1.5 (anti-CD4), 53-6.7 (anti-CD8), 331 (anti-IgM), 11-26 (anti-IgD), 6C31BP1 (anti-BP-1) and B3-B4 (CD23). mAbs against B220, CD19, CD43, CD24, CD5, CD21, IgM (Igh-6a), TCRβ, CD4, CD8, NK1.1, CD11b, CD11c, Gr-1, Ki67, phospho-phospholipase gamma 2 (PLCγ2) (pY759), phospho-spleen tyrosine kinase (Syk) (pY351) and isotype controls were purchased from BD Pharmingen (San Diego, CA, USA). Goat F(ab')$_2$ anti-mouse IgM and IgG fragments were purchased from Jackson Immunoresearch (West Grove, PA, USA). Biotinylated antibodies were visualized with streptavidin-conjugated FITC, PE, Cy5.5 PE and Alexa594 (BD Pharmingen). Rabbit mAbs specific for phospho-nuclear factor-kappa B (NF-κB) (Ser536), phospho-extracellular signal-regulated kinase (Erk)1/2 (Thr202/Tyr204) and rabbit polyclonal IκB-α were purchased from Cell Signaling Technology, Danvers, MA, USA. Anti-actin antibody (clone C4) was purchased from (Millipore, Temecula, CA, USA). The complete list of antibodies used for flow cytometry is presented in supplementary Table S1 (available at *International Immunology* Online).

High-dimensional (11-color) flow cytometry

Peripheral blood (7–10 drops) was collected in 500 μl of 10 mM EDTA in PBS and incubated with 1 ml of 2% dextran in PBS for 2 h at 37°C. The supernatant was transferred to a fresh tube for red cell lysis. Bone marrow cells were harvested by flushing femurs and tibias into 1 ml PBS containing 2% fetal bovine serum. Other lymphoid tissues (spleen, thymus and lymph node) were harvested and pressed through 70-μm nylon cell strainer and suspended in 10 ml of PBS. Peritoneal cells were harvested by injection of 10 ml PBS into the peritoneal cavity of a recently sacrificed mouse, the abdomen was massaged for 1 min, and the PBS was withdrawn. To eliminate red blood cells, single-cell suspensions from different tissues were incubated with red cell lysis buffer (150 mM NH_4Cl) for 5 min and washed with 10 v of PBS (23).

Cells were stained with cocktails of fluorochrome-conjugated antibodies (supplementary Table S1 is available at *International Immunology* Online). Surface staining (23) and intracellular staining (24) were performed as described. 'Fluorescence-minus-one' controls were included to determine the level of non-specific staining and auto-fluorescence associated with subsets of cells in each fluorescence channel. For surface staining, propidium iodide was added to all samples before data collection to identify dead cells. For staining of fixed samples, dead cells were marked by LIVE/DEAD® Fixable Dead Cell Stain Kits (Molecular Probes, Eugene, OR, USA). Hi-dimensional (Hi-D) flow cytometry data were collected on a highly modified triple-laser FACS instrument. FlowJo software (TreeStar, San Carlos, CA, USA) was used for fluorescence compensation and analysis.

Measurements of intracellular-free Ca^{2+} ion

Cells were incubated for 30 min at 37°C with Ca^{2+}-sensitive dyes Indo-1 (2 μg ml^{-1}) (Molecular Probes) in loading buffer (1 mM calcium, 1 mM magnesium and 1% FCS in HBSS). Cells were washed once with loading buffer containing 2.5 mM probenecid (Molecular Probes), which blocks the efflux of intracellular dyes (25). For analysis of Ca^{2+} flux in different lymphocytes subsets, splenocytes or bone marrow cells were then stained with antibodies specific for B220, IgM, IgD, CD23, CD21 and TCRαβ. Before stimulation, lymphocytes were warmed in a 37°C water bath and then analyzed on a Vantage SE cytometer equipped with 350-nm laser (BD Biosciences, San Jose, CA, USA). Baseline intracellular Ca^{2+} was measured for 1 min followed by the addition of F(ab')$_2$ anti-mouse IgM plus F(ab')$_2$ IgG, as indicated, at a final concentration of 50 μg ml^{-1} and the response to the stimulation was recorded for additional 4 min. Intracellular calcium flux was determined by measurement of the ratio of 405–485 nm emission after excitation with a 350-nm UV laser, the data were analyzed by FlowJo software.

Phospho-flow analysis

Single-cell suspensions of splenocytes (2×10^6) were stimulated with anti-IgM (50 μg ml^{-1}) in a volume of 100 μl at 37°C for 1–60 min. The cells were then fixed for 10 min by the addition of 10 μl 16% PFA (1.6% final concentration). Fixed cells were washed with PBS containing 3% FCS and then permeabilized with 250 μl cold Perm Buffer III (BD Biosciences) for 10 min and washed with PBS containing 3% FCS followed by staining with the fluorochrome-conjugated antibodies Alexa Fluor 647-phospho-Syk, Alexa Fluor 488-phospho PLCγ2, Pacific Blue-B220 and PE-CD3. The stained samples were acquired in a LSR II flow cytometer (BD Biosciences) and analyzed by FlowJo software.

B cell purification

Splenic B cells were purified by positive selection using anti-B220 antibody-conjugated magnetic beads (BD Biosciences) according to the manufacturer's instruction. Briefly, single-cell suspensions were incubated with anti-B220 antibody magnetic beads for 30 min at 4–8°C and B220-positive cells were isolated using a strong magnetic field (BD Biosciences).

Western blot analysis

Purified B cells were stimulated, lysed using 1× SDS sample buffer, heat denatured, electrophoresed and subjected to immunoblotting. Filters were probed with anti-phospho-NF-κB, -phospho-Erk1/2k, IκB-α and β-actin.

Lymphocyte proliferation assays

Purified B cells were incubated with 1 μM carboxyfluorescein succinimidyl ester (CFSE; Invitrogen, Carlsbad, CA, USA) for 7 min in serum-free media at room temperature. Cells

were then washed three times with complete Iscove's Modified Dulbecco's Medium containing 10% FCS. CFSE-labeled B cells were plated in flat bottom 96-well plates at a density of 0.2×10^6 per well and were incubated with anti-IgM F(ab')$_2$ fragments or with LPS (Sigma, St Louis, MO, USA) in the presence of 10 ng ml^{-1} recombinant IL-4 (R&D Systems, Minneapolis, MN, USA) for 72 h. Cells were washed once with PBS, propidium iodide was added to eliminate dead cells and analyzed by flow cytometer. Cell divisions were quantified by CFSE dilution using FlowJo software.

Analysis of Ki67 expression

Purified B cells (2×10^6) were incubated with goat anti-IgM F(ab')$_2$ fragments or LPS. After 48 h, cells were harvested and washed once with PBS, fixed with 1 ml of cold ethanol at −20°C for 2 h, washed again with 15 v of PBS and stained with anti-Ki67 antibody (clone B56). Finally, cells were stained with 1 μg ml^{-1} 4′,6-diamidino-2-phenylindole and acquired on a FACS Vantage SE flow cytometer equipped with 350-nm UV laser and analyzed by FlowJo software.

Analysis of B cell activation markers

Purified B-lymphocytes (5×10^5) were cultured in 96-well flat bottom plates. The cells were stimulated with 12.5 μg ml^{-1} goat anti-mouse IgM F(ab')$_2$ fragments, 1 μg ml^{-1} LPS, 5 μg ml^{-1} CpG (ODN1826) and 10 ng ml^{-1} IL-4. Expression of the indicated surface proteins was measured by flow cytometry after 24 h.

Bone marrow reconstitution of the lymphoid system in Rag1$^{-/-}$ mice

Single-cell suspensions of 2×10^6 whole bone marrow mononuclear cells from the indicated donor mice were injected intravenously into lethally irradiated (900 cGy, using a 200 Kv X-ray source) 8-week-old male *Rag1*$^{-/-}$ recipient mice. Peripheral blood from the chimeric mice was used to monitor the reconstitution of B and T cells, as detailed above.

Adoptive transfer of B cells to Rag1$^{-/-}$ recipients

Purified B cells (20×10^6) from donor spleens were injected intravenously into the sub-lethally irradiated (300 cGy) 8-week-old male *Rag1*$^{-/-}$ recipient mice.

Immunizations and analysis of immune responses

Mice were immunized by intra-peritoneal injection of 50 μg 2,4,6, trinitrophenol (TNP)–LPS (Biosearch Technologies, Novato, CA, USA). TNP-specific antibodies in the sera of the immunized mice were determined by ELISA. TNP–BSA (Biosearch Technologies) was used as the capture antigen and the reactivity detected by the isotype specific antibodies (Southern Biotech, Birmingham, AL, USA).

Statistical analysis

P values were determined by applying Student's two-tailed *t*-test for independent samples assuming equal variances on all experimental data sets.

Results

Increased Ca^{2+} influx in CD81-deficient B cells upon BCR induction

One of the early events in B cell activation is an increase in intracellular-free calcium ion (26). To test the role of CD81 in B cell activation, we stimulated cells via their BCR. Splenocytes from *Cd81*$^{-/-}$ and wild-type littermate mice were loaded with the calcium ion sensitive dye Indo-1. The cells were then stained with antibodies against different lymphocyte markers and activated by anti-BCR F(ab')$_2$ fragments. Intracellular-free calcium was measured by flow cytometry. In our experiments, *Cd81*$^{-/-}$ B cells (B220$^+$) displayed a markedly increased influx of Ca^{2+} ion upon BCR stimulation compared with B cells from wild-type littermates (Fig. 1A). In these studies, T cells (TCR$\alpha\beta^+$) serve as an important internal negative control and indeed showed no increase in intracellular-free Ca^{2+} under these anti-BCR stimulation conditions (Fig. 1B).

We performed a more detailed analysis and found that most splenic B cell subsets from *Cd81*$^{-/-}$ mice had an increased Ca^{2+} influx compared with wild-type B cells (Fig. 1C). The most prominent increase was observed in follicular B cells (the majority of B cells in the spleen). However, all mature *Cd81*$^{-/-}$ B cells (marginal zone, mixed B cells comprising follicular and B1) had increased Ca^{2+} influx, whereas a subset containing immature (transitional) B cells and some B1 cells was refractory to BCR induction in either genotype. The mature IgM$^+$IgD$^+$ B cells in the bone marrow also responded with increased Ca^{2+} ion influx (as detailed later, Fig. 6B).

There was no difference in the representation of the mature B cell subsets between *Cd81*$^{-/-}$ and wild-type mice in the spleen, lymph nodes and in the peritoneum (supplementary Figure S1 is available at *International Immunology* Online). However, there were fewer splenic immature B cells in *Cd81*$^{-/-}$ mice (Fig. 1C).

Increased phosphorylation of signaling molecules in Cd81$^{-/-}$ B cells responding to BCR engagement

To determine whether the signaling pathways downstream of the BCR were enhanced in *Cd81*$^{-/-}$ B cells, we analyzed the phosphorylation of Syk, a BCR proximal kinase. We stimulated splenocytes with anti-IgM antibodies and analyzed the phosphorylation of Syk in both B and T cells by flow cytometry (24). *Cd81*$^{-/-}$ B cells showed increased phosphorylation of Syk compared with wild-type littermate B cells (Fig. 2A, C and E). Again, the T cell population served as an internal negative control and showed no increase in signal, demonstrating the specificity of the phospho-flow assay.

We also examined the activation of PLCγ2, which sustains B cell activation by generating inositol-1,4,5-triphosphate and diacylglycerol that, in turn, affects the concentration of cytosolic Ca^{2+} ions and initiates a positive feedback loop to maintain B cell activation (27). BCR induction led to increased phosphorylation of PLCγ2 in *Cd81*$^{-/-}$ B cells compared with their wild-type counterparts (Fig. 2B, D and E). Therefore, our results show that, in the absence of CD81, stimulation of B cells via BCR led to enhanced early B cell activation events including both an increase in intracellular-free

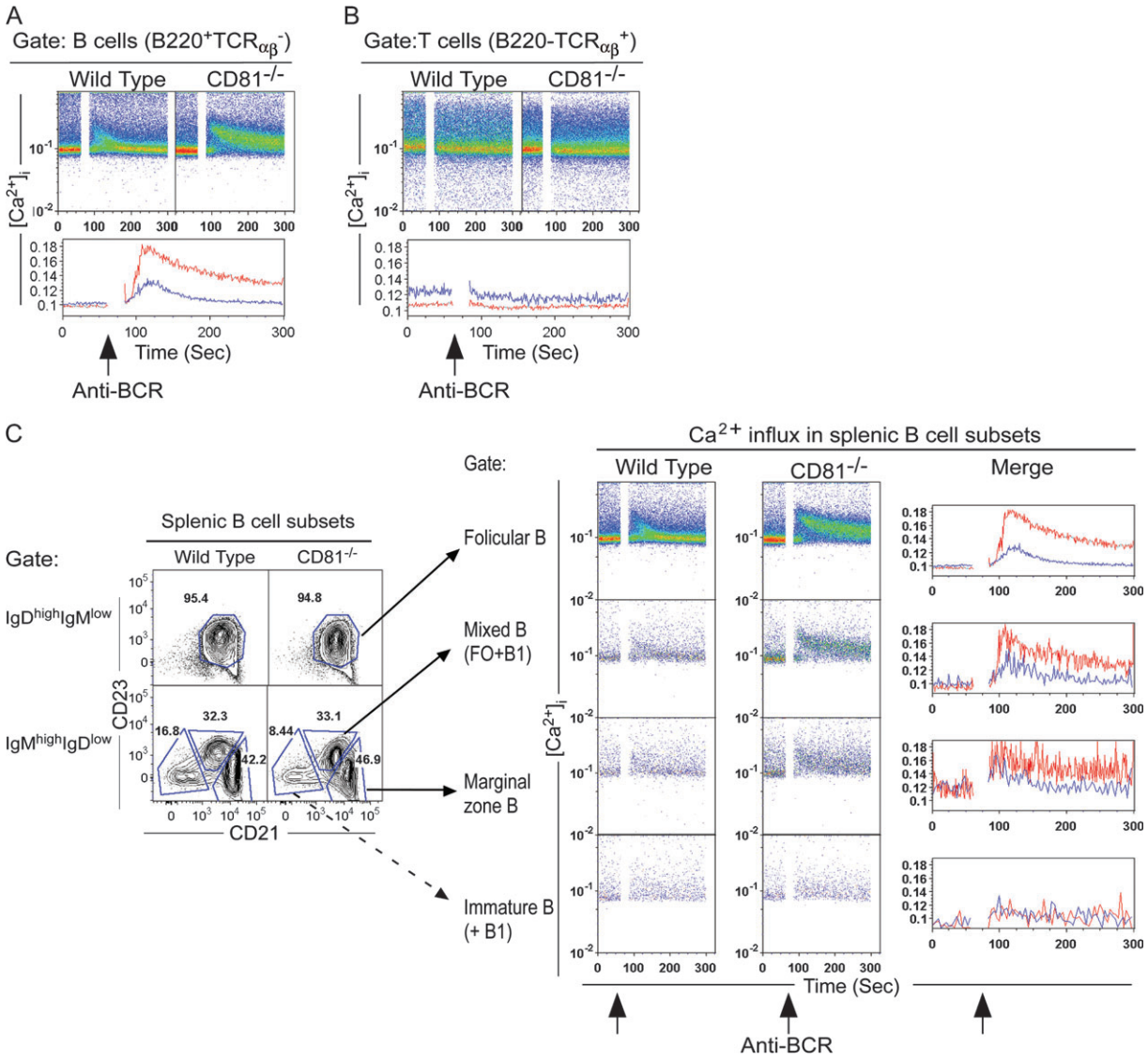

Fig. 1. Enhanced BCR-induced Ca^{2+} influx in *Cd81*$^{-/-}$ B cells. Spleen cells were loaded with Ca^{2+}-sensitive dye, indo-1 followed by staining with fluorochrome-conjugated antibodies against the indicated B and T cell markers and intracellular-free calcium ion was measured by flow cytometry. (A) B cells were stimulated with $F(ab')_2$ anti-IgM plus $F(ab')_2$ anti-IgG (50 μg ml^{-1}). Top panels show influx of Ca^{2+} ion in $B220^+$ cells as a ratio of fluorescence at 405–485 nm emissions as a function of time. Bottom panels show the merged kinetics of influx of Ca^{2+} in wild-type (blue) and *Cd81*$^{-/-}$ (red) B cells. Shown are representative of 10 independent experiments. (B) Note that $TCR\alpha\beta^+$ did not flux Ca^{2+} in this stimulation condition. (C) Splenic B cell subsets were resolved by fluorochrome-conjugated antibodies. Influx of Ca^{2+} ion in wild-type (left column panels) and *Cd81*$^{-/-}$ (middle column panels) B cell subsets (gated as indicated) are shown. The merged kinetics of wild-type (blue) and *Cd81*$^{-/-}$ (red) B cells are shown in the right column panels. All *Cd81*$^{-/-}$ splenic B cell subsets had an increased influx of Ca^{2+} ion upon BCR stimulation.

calcium ion and an increase in the phosphorylation of the downstream signaling kinases.

Increased proliferation of Cd81$^{-/-}$ *B cells in response to activation*

Previous analyses of the proliferative response of *Cd81*$^{-/-}$ B cells have been inconsistent (17, 18). Therefore, we purified B cells from *Cd81*$^{-/-}$ or wild-type littermates, labeled them with CFSE, stimulated them with anti-IgM antibody and analyzed cell division by flow cytometry. This stimulation resulted in a moderate increase in proliferation of *Cd81*$^{-/-}$ B cells (Fig. 3A). In order to address whether this effect was restricted to activation via the BCR, we stimulated the B cells with LPS (28) to activate the TLR4 pathway. Stimulation by LPS induced a pronounced increase in the proliferation of *Cd81*$^{-/-}$ B cells (Fig. 3A). These results were confirmed by examining the expression of the proliferation-associated nuclear protein Ki67 (29). The fraction of cycling *Cd81*$^{-/-}$ B cells was higher than that of wild-type B cells stimulated either by anti-IgM or by LPS (Fig. 3B).

B cell activation and proliferation are generally associated with increased expression of co-stimulatory molecules (30). Initially, we compared the basal levels of CD80, CD86 and CD69 in resting B cells and found no difference between

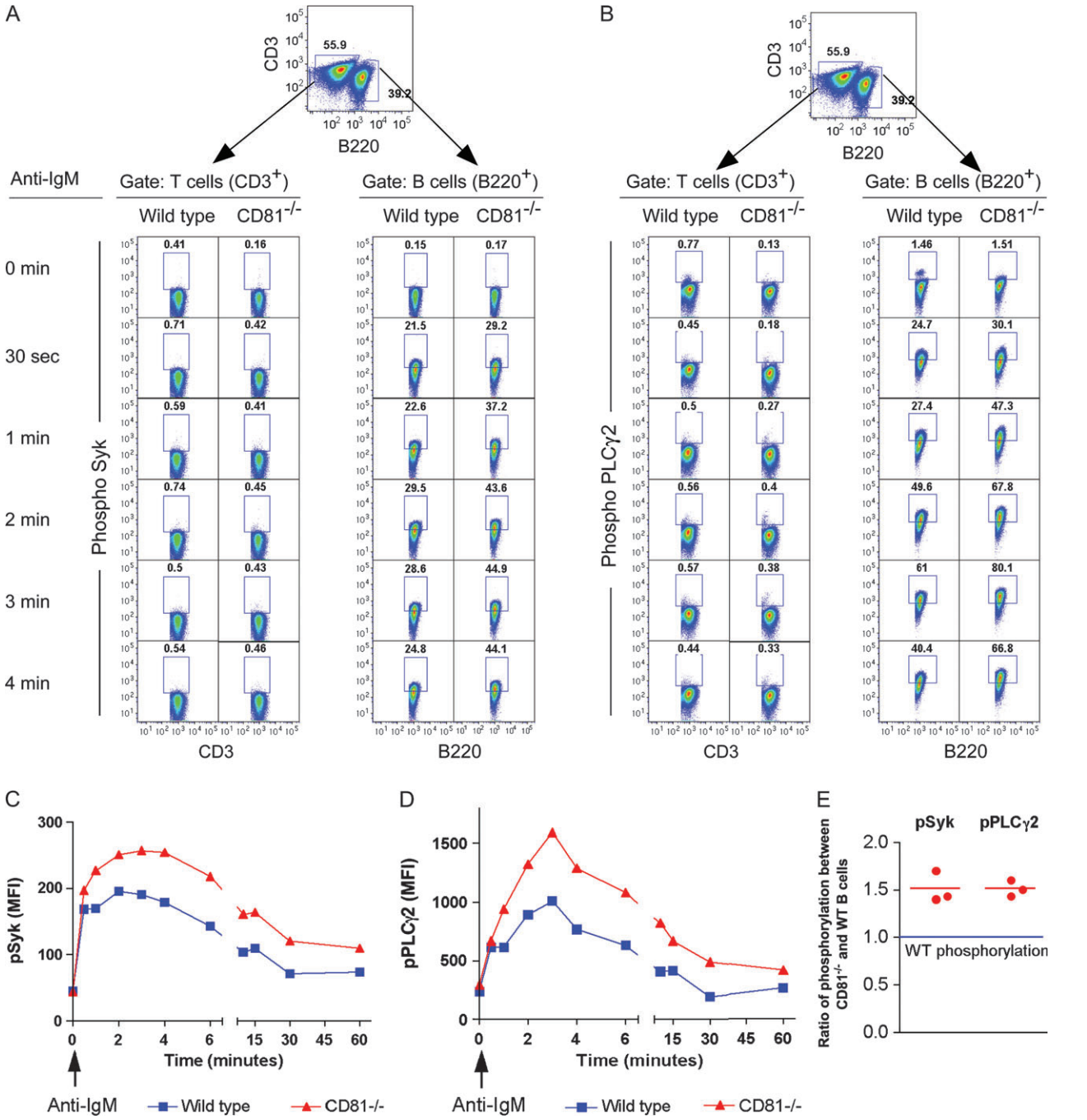

Fig. 2. BCR-induced phosphorylation of Syk and PLCγ2 is increased in *Cd81*$^{-/-}$ B cells. Splenocytes were stimulated with F(ab')$_2$ anti-IgM (50 μg ml^{-1}) for the indicated time periods at 37°C, control cells were left unstimulated (0'). After stimulation, cells were fixed, permeabilized and stained with fluorochrome-conjugated anti-B220, CD3 and phospho-Syk (A), phospho-PLCγ2 (B) antibodies and analyzed by flow cytometry. The respective phosphoprotein staining in wild-type and *Cd81*$^{-/-}$-gated CD3$^+$ and B220$^+$ cells in unstimulated (0') and in the initial 4 min after stimulation are shown. Boxes indicate the percentages of positive cells above unstimulated cells. (C) Mean fluorescence intensities of phospho-Syk and phospho-PLCγ2 (D) staining in wild-type (blue) and *Cd81*$^{-/-}$ (red) B cells (B220$^+$) as function of time are plotted. These data represent three independent experiments. (E) Ratio of phosphorylation of Syk and PLCγ2 in B cells between *Cd81*$^{-/-}$ and wild-type after 3 min of stimulation from three independent experiments.

Cd81$^{-/-}$ and wild-type resting B cells (Fig. 4A). We then purified B cells and activated them via the BCR, TLR4 and TLR9 pathways and by IL-4. Each of these stimuli increased the expression of CD86 and CD69 comparably in *Cd81*$^{-/-}$ and wild-type B cells (Fig. 4).

BCR- and TLR-mediated signaling pathways have certain aspect in common, but rely on distinct proximal signaling effectors. To address whether TLR-mediated signaling in *Cd81*$^{-/-}$ B cells was enhanced, we stimulated purified B cells with LPS and analyzed the activation of the NF-κB pathway. This analysis

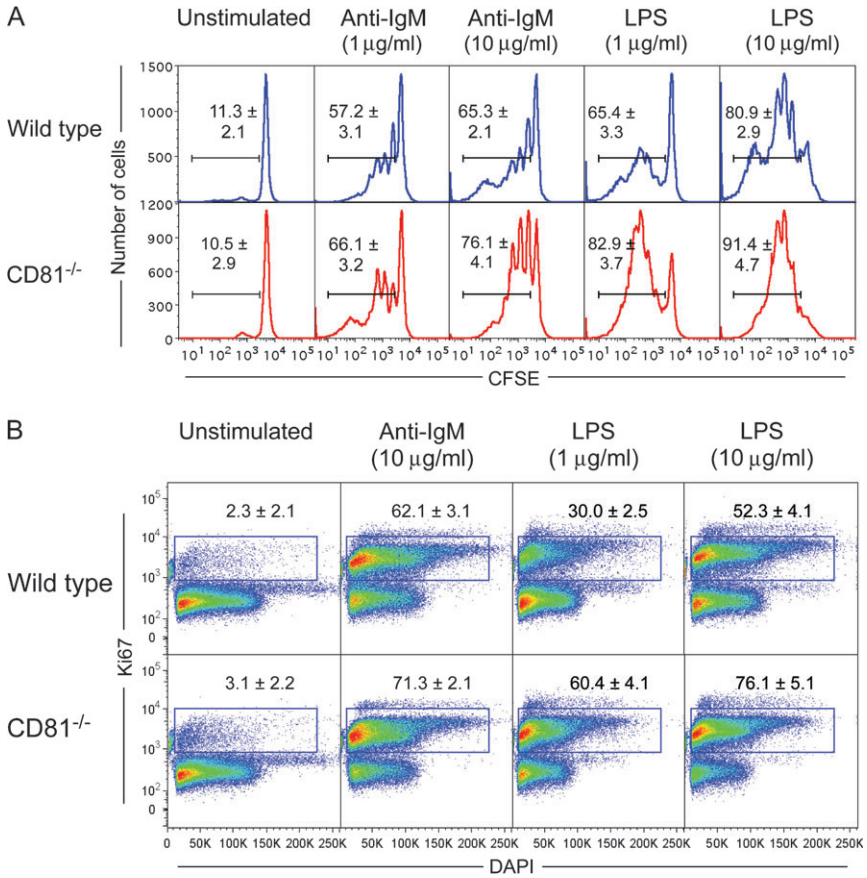

Fig. 3. Increased proliferation in activated *Cd81*$^{-/-}$ B cells. (A) Purified B cells from wild-type and *Cd81*$^{-/-}$ mice were labeled with 1 μM CFSE and cultured for 72 h in the presence of IL-4 (10 ng ml^{-1}) and the indicated amounts of anti-IgM F(ab')$_2$ and LPS. Cellular proliferation was analyzed by flow cytometry. CFSE dilution in gated live cells is shown. Histograms of one of four independent experiments are shown. The percentages of proliferating cells in these experiments are indicated as mean ± SD. (B) Purified B cells from wild-type and *Cd81*$^{-/-}$ mice were stimulated for 48 h with the indicated amounts of anti-IgM F(ab')$_2$ or LPS in presence of 10 ng ml^{-1} IL-4. Following stimulation, lymphocytes were fixed, permeabilized and stained with FITC-conjugated anti-Ki67 antibody and 4′,6-diamidino-2-phenylindole (DAPI). Ki67^{+} cells indicated by the box represent all cycling cells including (G_1, G_2, M plus S stages). Dot plots from one of four independent experiments are shown; the percentages of cycling cells in these experiments are indicated as mean ± SD.

showed a moderate increase in IκB-α degradation along with a concomitant increase in phosphorylation of NF-κB in *Cd81*$^{-/-}$ B cells (supplementary Figure S2A is available at *International Immunology* Online). In addition, phosphorylation of Erk1/2 was initiated earlier and moderately enhanced in *Cd81*$^{-/-}$ in comparison with wild-type B cells (supplementary Figure S2B is available at *International Immunology* Online).

Lack of CD81 in the environment does not influence the Cd81$^{-/-}$ *B cell phenotype*

CD81 is widely expressed and therefore a possibility exists that the observed hyperactive phenotype is the result of an influence by CD81-deficient environment on the developing B cells. To address this possibility, we transplanted bone marrow from *Cd81*$^{-/-}$ or wild-type animals into *Rag1*$^{-/-}$ mice (Fig. 5A). The bone marrow of both genotypes reconstituted B and T cell compartments similarly (data not shown). B cells arising from *Cd81*$^{-/-}$ donors had reduced expression of CD19, similar to that seen in *Cd81*$^{-/-}$ mice (Fig. 5B) (16–18) demonstrating that CD19 reduction is an intrinsic property of the *Cd81*$^{-/-}$ donor cells.

We then purified the B cells (*Cd81*$^{-/-}$ and wild-type) that had regenerated in the *Rag1*$^{-/-}$ environment and analyzed their response to stimulation by anti-IgM and LPS. The proliferation in response to these stimuli was differentially enhanced in the *Cd81*$^{-/-}$ B cells recovered from the *Rag1*$^{-/-}$ hosts (Fig. 5C). We also measured LPS-induced IgM secretion in these purified B cells. *Cd81*$^{-/-}$ B cells obtained from *Rag1*$^{-/-}$ chimeras secreted significantly higher amounts of IgM than the wild-type B cells (Fig. 5D). A similar increase in IgM secretion was observed in donor *Cd81*$^{-/-}$ B cells (Fig. 5D). Thus, enhanced sensitivity to activation is not dependent upon the CD81-deficient environment in which these *Cd81*$^{-/-}$ B cells naturally arise.

The bone marrow of Cd81$^{-/-}$ *mice has increased IgM*$^{+}$*IgD*$^{+}$ *cells*

Mice lacking negative regulators of B cell activation, such as CD22 and CD72, frequently have fewer mature B cells in their bone marrow (31). We therefore analyzed mature B cell subsets in all lymphoid locations. Spleen (Fig. 1C), lymph nodes and peritoneal cavity (supplementary Figure S1 is available at *International Immunology* Online) of *Cd81*$^{-/-}$

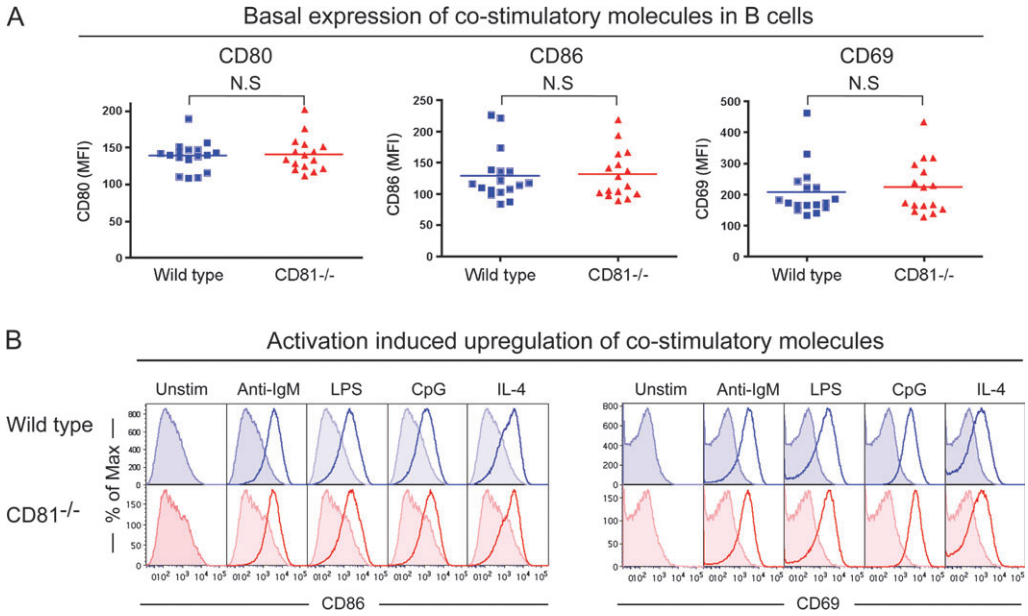

Fig. 4. Expression of co-stimulatory molecules in resting and activated *Cd81*$^{-/-}$ and wild-type B cells. (A) PBMC from *Cd81*$^{-/-}$ and wild-type mice were stained with fluorochrome-conjugated anti-CD80, CD86 and CD69 antibodies and analyzed by flow cytometry. Mean fluorescent intensities of CD80, CD86 and CD69 staining in individual mice are plotted, median values are shown by horizontal lines; the difference in mean values are not statistically significant ($N = 20$). (B) Expression of CD86 and CD69 after overnight culturing of purified B cells in the presence of anti-IgM (12.5 μg ml^{-1}), LPS (10 μg ml^{-1}), TLR9 agonist CpG (ODN1826) at 5 μg ml^{-1} or IL-4 (10 ng ml^{-1}). Shaded and open histograms represent the expression of the respective markers in the unstimulated B cells and the stimulated cells, respectively. These data are representative of five independent experiments.

and wild-type mice had similar, normal, representation of all these subsets. However, in the bone marrow B220^{+}CD43^{-}IgM^{+}IgD^{+} B cells, corresponding to Hardy fraction F (32) were over-represented in *Cd81*$^{-/-}$ mice (Fig. 6A). These are the most mature B cells in the bone marrow and express high CD21 levels, similar to splenic marginal zone B cells (33). Stimulation of the BCR in these cells resulted in increased Ca^{2+} ion influx in *Cd81*$^{-/-}$ cells compared with their wild-type counterparts (Fig. 6B), similar to that seen with *Cd81*$^{-/-}$ splenic B cells (Fig. 1). We also sorted bone marrow IgM^{+}IgD^{+} B cells (Fig. 6C, left panels) and stimulated them with LPS; once again, those derived from *Cd81*$^{-/-}$ mice secreted significantly higher amounts of IgM compared with their wild-type counterparts (Fig. 6C).

Increased T-independent immune response in Cd81$^{-/-}$ *mice*

The foregoing results demonstrated an ability of *Cd81*$^{-/-}$ B cells to be hyperactivated upon BCR or LPS stimulation. The analysis of a large cohort of mice revealed that the serum levels of IgM, IgG_3 and IgG were not significantly different between wild-type or *Cd81*$^{-/-}$ mice (Fig. 7A–C, respectively). However, when immunized with the T-independent antigens, TNP–LPS and TNP–ficoll, *Cd81*$^{-/-}$ mice responded with an elevated primary TNP-specific IgM immune response, compared with wild-type mice (Fig. 7D and supplementary Figure S3 is available at *International Immunology* Online, respectively). The mice were boosted after the primary immune response subsided, and the analysis of the secondary immune response showed significantly elevated levels of IgM, IgG_3 and IgG anti-TNP antibodies in the serum of *Cd81*$^{-/-}$ mice (Fig. 7D).

We then purified splenic B cells from *Cd81*$^{-/-}$ and from wild-type mice and adoptively transferred them to *Rag1*$^{-/-}$ mice (Fig. 7E). The adoptively transferred animals were reconstituted with B cells, but lacked T cells, as expected. Also, as expected, the reconstituted *Cd81*$^{-/-}$ B cells expressed lower levels of CD19 than their wild-type counterparts (Fig. 7F, lower panels). The mice were immunized 7 days after the adoptive transfer with TNP–LPS, followed by analysis of TNP-specific IgM response. The mice reconstituted with *Cd81*$^{-/-}$ B cells mounted a higher antigen-specific T-independent immune response (Fig. 7G), as was the case in the *Cd81*$^{-/-}$ donor animals. These *in vivo* results are consistent with an intrinsic ability of *Cd81*$^{-/-}$ B cells to overrespond to direct stimulation and they are consistent with all of our *in vitro* studies on these *Cd81*$^{-/-}$ B cells.

Discussion

Our current study demonstrates that in the absence of CD81, B cells display a hyperactive phenotype in response to stimulation *in vitro* and *in vivo*. This phenotype was transferable to *Rag*$^{-/-}$ host and was not dependent upon the CD81-deficient stromal environment. Based on these results, we propose that CD81 serves as a negative regulator of B cell activation.

CD81 was shown to associate with lipid rafts upon co-ligation of the BCR and the CD19/CD21 complex, whereas in the absence of CD81, these two complexes failed to partition into lipid rafts (34). This biochemical study pointed to a role of CD81 in amplifying and prolonging BCR signaling from lipid rafts via co-receptor CD19/CD21 complex.

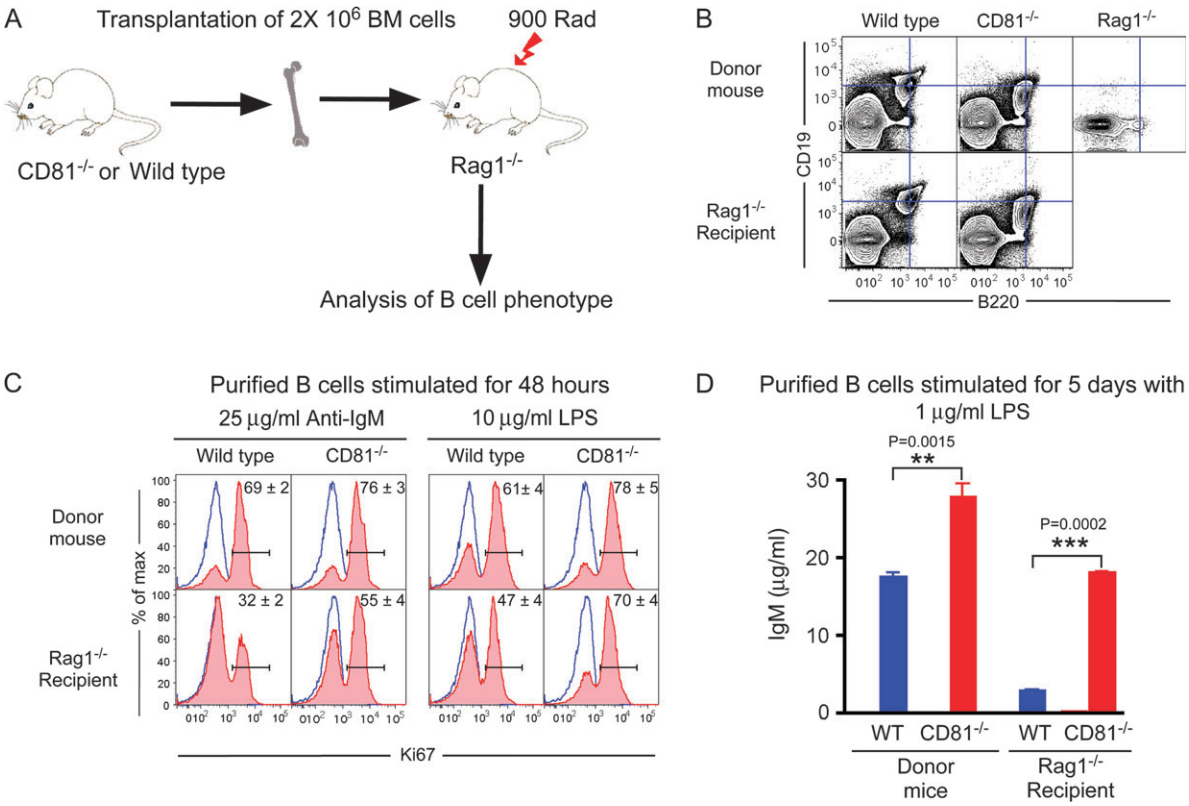

Fig. 5. The *Cd81*$^{-/-}$ B cell phenotype is not due to CD81-deficient stromal environment. (A) Schema of bone marrow transplantation into *Rag1*$^{-/-}$ mice. Bone marrow cells were isolated from 8-week-old wild-type or *Cd81*$^{-/-}$ mice. A total of 2 × 10^6 bone marrow cells were injected into lethally irradiated *Rag1*$^{-/-}$ mice via tail vein. Analysis of the peripheral blood of the recipients by flow cytometry monitored reconstitution of the lymphoid system. (B) Spleen cells from *Rag1*$^{-/-}$ chimeric mice (10 weeks post-transplant) and primary control mice were stained with fluorochrome-conjugated anti-B220 and anti-CD19 antibody. Note the reduced CD19 expression levels in *Cd81*$^{-/-}$ B cells both in primary and *Rag1*$^{-/-}$ chimeric mice. (C) B cells were purified from primary or *Rag1*$^{-/-}$ chimeric mice. B cells (2 × 10^6) were cultured for 48 h in presence of anti-IgM or LPS, fixed, permeabilized and stained with the anti-Ki67 antibody. Histograms are shown as overlay of Ki67 expression in unstimulated (blue line) and stimulated (red tinted area) B cells from the indicated mice. The histograms shown are of one of three independent experiments; the percentages of proliferating cells in these experiments are indicated as mean ± SD. (D) Purified B cells from the indicated mice were cultured for 5 days in presence of LPS (1 µg ml^{-1}) and the secreted IgM was measured by ELISA. There was a significant difference in IgM secretion between *Cd81*$^{-/-}$ and wild-type-stimulated B cells, obtained from the primary and *Rag1*$^{-/-}$ chimeric mice (*N* = 3; *P* values for each group are indicated).

However, our current results do not validate this prediction (Figs 1–3 and 7).

The partnership of CD81 with CD19 was originally demonstrated in human B cells, where the two molecules co-precipitated each other (8). CD19 is expressed very early during B cell development at Hardy fraction B (35, 36, 55). However, the onset of CD81 expression during B cell development was not known. Our current analysis shows that the onset of CD19 expression coincides with that of CD81 during early B cell development (supplementary Figure S4 is available at *International Immunology* Online). Interestingly, three independently derived *Cd81*$^{-/-}$ mice have reduced CD19 expression (16–18). Therefore, it is likely that the expression of CD19 and CD81 are regulated at the early stage of B cell development during the initial assembly of the co-receptor complex. In support of this, our previous study showed that CD81 is involved in intracellular trafficking of CD19 to the cell surface; subsequently, we identified the structural domains within the CD81 molecule required for cell surface expression of CD19 (21).

Since the expression of CD81 and CD19 are so intimately linked, it is important to distinguish the individual contribution to the B cell hyperactivity associated with CD81 deficiency that we have observed here. Natural mutation of CD19 in human (37, 38) or engineered knockout mutations in mice (13, 39) result in profound deficiency in response to BCR activation. In human, the mutation of CD19 leads to reduced immune response (37, 38). *Cd19*$^{-/-}$ mice lack germinal centers and have a deficiency in affinity maturation of antibodies (40). In addition, *Cd19*$^{-/-}$ mice expressing human CD19 without the cytoplasmic signaling domain also display reduced immune responses (14). The original assessment of the function of CD19 by ligation with an antibody reported an inhibitory effect (41), later it was shown that this effect is dependent on the system used, as independent ligation of CD19 inhibited BCR-induced B cell activation (41, 42), whereas co-cross-linking of CD19 and the BCR was stimulatory (11, 42). In addition, a sustained increase in BCR-induced calcium influx in CD19-defficient B cells was reported (12, 14); however, these studies failed to

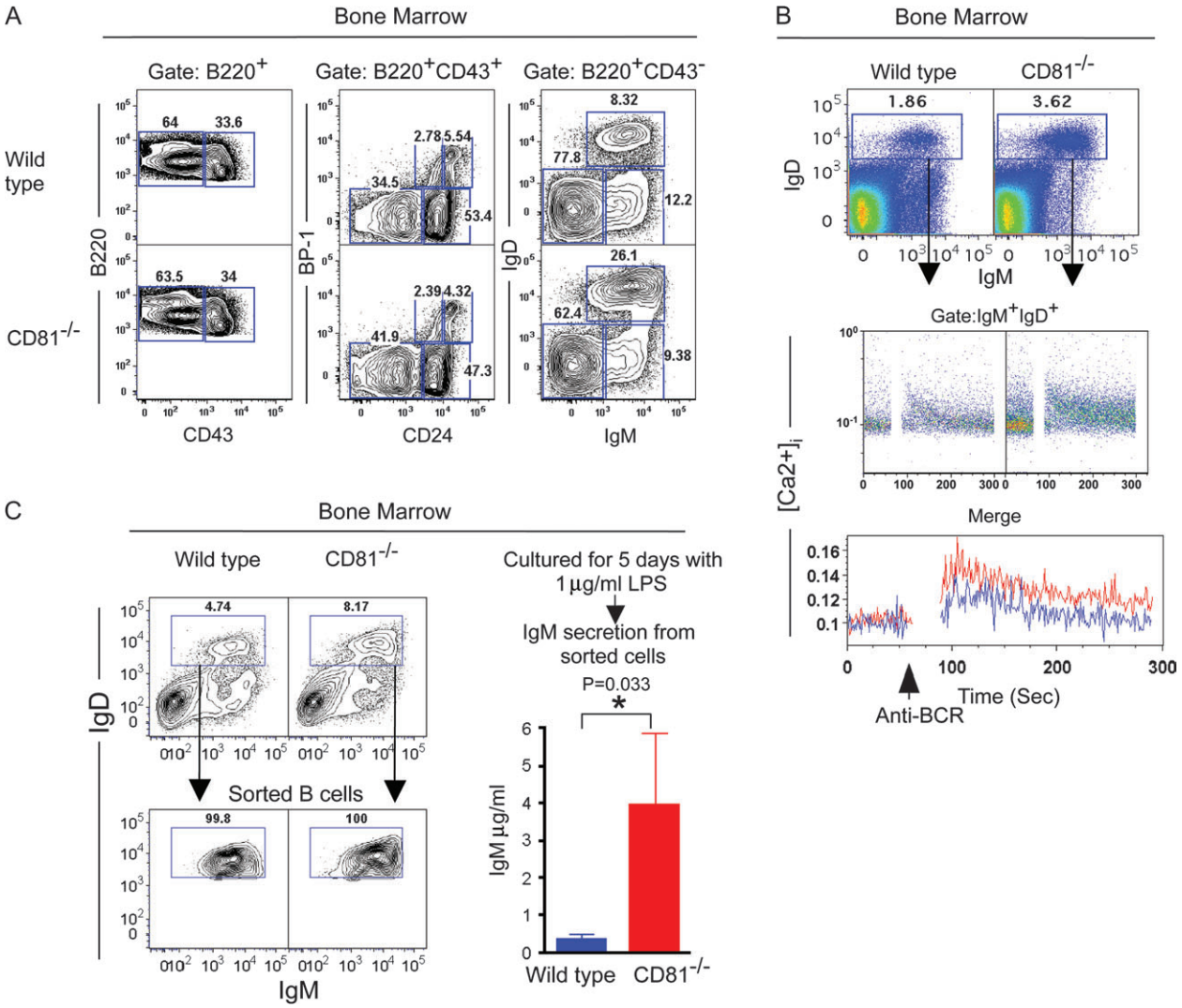

Fig. 6. The mature B cell subset (IgM^+IgD^+) is increased in the bone marrow of *Cd81*$^{-/-}$ mice. (A) Bone marrow cells were stained with fluorochrome-conjugated anti-B220, CD43, BP-1, IgM and IgD antibodies (32). Cells corresponding to fraction F (IgM^+IgD^+) are increased in *Cd81*$^{-/-}$ bone marrow. (B) Bone marrow cells were loaded with the calcium sensitive dye Indo-1 and stained with fluorochrome-conjugated IgM and IgD antibodies. Cells were stimulated with anti-IgM plus IgG (50 µg ml^{-1}) and intracellular-free Ca^{2+} ion was measured by flow cytometry. IgM^+IgD^+ B cells in *Cd81*$^{-/-}$ (red) bone marrow showed an increased influx of $Ca2^+$ ion upon BCR stimulation. (C) Increased antibody secretion from *Cd81*$^{-/-}$ IgM^+IgD^+ cells. Bone marrow cells were stained with fluorochrome-conjugated anti-IgM and anti-IgD antibodies and IgM^+IgD^+ cells were sorted (as shown in the left panels). Equal numbers of sorted cells from the *Cd81*$^{-/-}$ and wild-type bone marrow were cultured for 5 days in the presence of 1 µg ml^{-1} LPS (N = 3 for each group). IgM secretion measured from the spent media was significantly different (right panel).

reflect increase in downstream signaling. Despite these discrepancies, overall CD19 is reported to enhance BCR-mediated intracellular signaling (11–15, 43). Therefore, reduced CD19 expression in *Cd81*$^{-/-}$ B cells would have been expected to lead to reduced ability to be activated. However, we show here that *Cd81*$^{-/-}$ B cells are hyperresponsive. Hence, it is most likely that hyperresponsiveness of CD81-deficient B cells upon activation cannot be attributed *per se* to reduced CD19 levels.

Engagement of the BCR results in an increase in cytosolic-free calcium ion (27). Previously, Tsitsikov *et al.* (18) reported normal calcium influx in response to BCR ligation in *Cd81*$^{-/-}$ B cells. Here, we re-examined BCR-induced calcium response in a large cohort of *Cd81*$^{-/-}$ mice and consistently observed an increased influx of calcium ion compared with wild-type controls (Fig. 1). Another hallmark of early B cell activation is the phosphorylation of downstream kinases (44). Consistent with the increased Ca^{2+} influx, the phosphorylation of Syk, the proximal signaling kinase downstream of BCR and PLCγ2 that stabilizes B cell activation were increased in *Cd81*$^{-/-}$ B cells (Fig. 2). Our result differs from that summarized without presentation of their data by Miyazaki *et al.* (17), claiming that BCR-induced calcium response is unaffected in *Cd81*-deficient B cells. Our data clearly demonstrate that lack of CD81 leads to enhanced early B cell activation events in response to stimulation of the BCR (Figs 1 and 2).

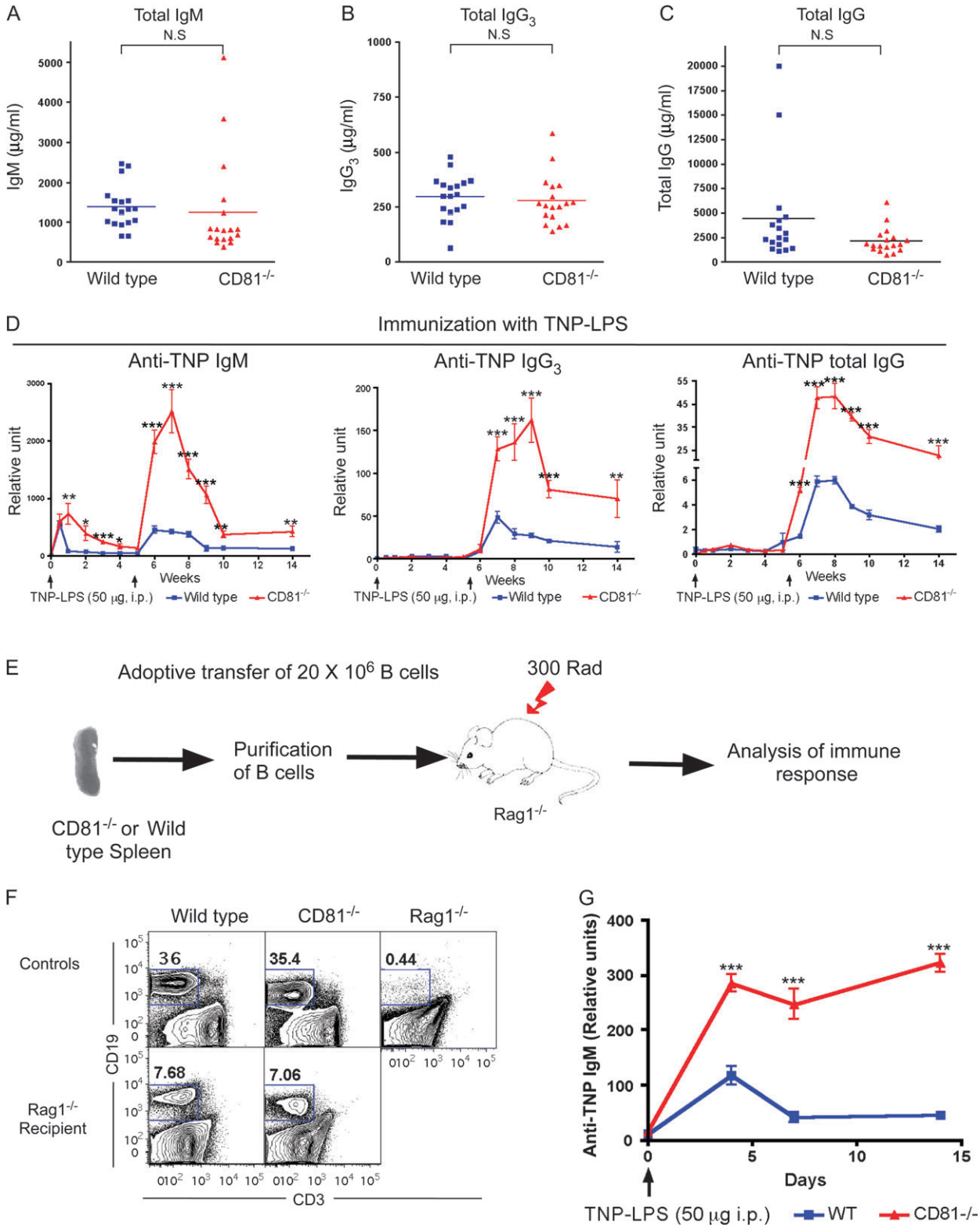

Fig. 7. Increased immune response to a T-independent antigen in *Cd81*$^{-/-}$ mice. Basal serum IgM (A), IgG_3 (B) and IgG (C) level in wild-type (blue) and *Cd81*$^{-/-}$ (red) mice, median values are shown by horizontal lines; the difference in mean values are not statistically significant ($N = 18$). (D) Wild-type ($N = 6$) and *Cd81*$^{-/-}$ ($N = 6$) mice were immunized intra-peritoneally with TNP–LPS (50 µg ml^{-1}) and boosted 5 weeks after the initial immunization. Pre-immune and post-immune sera were collected and TNP-specific IgM (left), IgG_3 (middle) and total IgG (right) were measured by ELISA. Plotted is the response of wild-type (blue) and *Cd81*$^{-/-}$ (red) mice as mean ± SD. Significance of differences in mean values for the indicated time points are shown by asterisk (*$P \leqslant 0.05$, **$P \leqslant 0.001$ and ***$P \leqslant 0.0001$). (E) Adoptive transfer of B cells. B cells were purified from wild-type or the *Cd81*$^{-/-}$ spleen based on B220 staining. A total of 20×10^6 B cells were injected to sub-lethally irradiated

Past reports on the proliferative responses of *Cd81*$^{-/-}$ B cells to different stimuli resulted in conflicting results. For example, Miyazaki *et al*. (17) reported increased proliferation in response to stimulation by LPS but decreased proliferation in response to stimulation by immobilized anti-IgM. Whereas, Tsitsikov *et al.* (18) showed normal proliferation using soluble anti-IgM reported. Our re-analysis showed a mild increase in proliferation of *Cd81*$^{-/-}$ B cells in response to BCR stimulation (Fig. 3). The increased proliferative capacity of *Cd81*$^{-/-}$ B cells was even more apparent in response to activation of the TLR4 pathway by LPS (Fig. 3). We confirmed this increase in proliferation by measuring Ki67 expression in cycling cells (Fig. 3B). We further observed that activation of TLR4 pathway via LPS led to a moderate increase in intracellular signaling in *Cd81*$^{-/-}$ B cells (supplementary Figure S2 is available at *International Immunology* Online).

B cell activation is associated with the up-regulation of several co-stimulatory molecules. Analysis of the levels of CD80, CD86 and CD69 in resting and activated B cells showed no difference in their expression between *Cd81*$^{-/-}$ and wild-type cells (Fig. 4). Thus, once activated, *Cd81*$^{-/-}$ B cells equally express the co-stimulatory molecules required for interaction with T cells. However, our previous studies have demonstrated that cognate interaction between *Cd81*$^{-/-}$ B and T cells result in impaired T_h2 immune responses *in vitro* and *in vivo* (45, 46).

Previous analyses of humoral response of the three *Cd81*$^{-/-}$ lines differed considerably in the antigens and schedules used (16–18). To focus specifically on the B cell response *in vivo*, we used T-independent antigens. In agreement with the *in vitro* data (Figs 1–3, 5), we found that *Cd81*$^{-/-}$ mice mounted stronger immune responses, both to primary (IgM) and to secondary (IgM, IgG_3 and IgG) booster vaccinations (Fig. 7D, supplementary Figure S3 is available at *International Immunology* Online). When splenic B cells were adoptively transferred to *Rag1*$^{-/-}$ mice, those receiving *CD81*$^{-/-}$ cells (Fig. 7F) also showed enhanced immune response to TNP–LPS (Fig. 7G).

CD81 is widely expressed; therefore, multiple cellular interactions might influence the specific cell type analyzed. It was previously shown that CD81 in stromal cells was required for the development of T cells in fetal organ tissue culture (47). We therefore tested whether the hyperactive *Cd81*$^{-/-}$ B cell phenotype could also be influenced by the *Cd81*$^{-/-}$ stromal environment during B cell development. We transferred bone marrow cells into *Rag1*$^{-/-}$ recipients and analyzed the donor-derived B cells (Fig. 5A). Functionally, these B cells exhibited the same hyperactive phenotype in response to stimulation, including increased proliferation (Fig. 5C) and increased IgM secretion (Fig. 5D), as did primary *Cd81*$^{-/-}$ B cells. These results provide evidence that a CD81-deficient stromal environment does not influence the *Cd81*$^{-/-}$ B cell phenotype.

Altered B cell activation could be associated with B cell developmental abnormalities (48). However, analysis of the lymphoid compartments in *Cd81*$^{-/-}$ primary mice and in the chimeric *Cd81*$^{-/-}$*Rag1*$^{-/-}$ mice generated by bone marrow transplantation did not show differences in B cell subsets in the spleen and lymph nodes (supplementary Figure S1B and C is available at *International Immunology* Online). Interestingly, we noticed an over-representation of IgM^+IgD^+ B cells in the bone marrow of *Cd81*$^{-/-}$ mice (Fig. 6A). IgM^+IgD^+ B cells (Hardy fraction F) (32) represent the mature B cell subset in the bone marrow. These cells reside in the perisinusoidal space of the bone marrow and participate in T-dependent humoral immune responses, providing the first line of defense against blood-borne pathogens (33). However, unlike their counterparts in the follicular niche, these cells are capable of being activated *in situ* by blood-borne microbes in a T-independent manner to generate specific IgM antibodies. These cells also represent a significant pool of B cells in the body (33). This IgM^+IgD^+ bone marrow population in *Cd81*$^{-/-}$ mice was hyperresponsive to BCR stimulation as evident by increased Ca^{2+} influx (Fig. 6B) and secreted higher amounts of IgM upon polyclonal stimulation with LPS (Fig. 6C). In contrast, mice lacking the negative regulators of B cell activation, i.e. Aiolos, the zinc finger DNA-binding protein (49), the cell surface molecules CD22 (50–52) and CD72 (53) have a common B cell maturation defect. They have fewer mature B cells in the bone marrow but normal B cell subsets in the secondary lymphoid organs. It was inferred that the lack of mature B cells in the bone marrow is linked to the lack of negative regulation of B cell activation (31). However, the situation is reversed in *Cd81*$^{-/-}$ mice, which exhibit a hyperactive B cell phenotype and have increased representation of IgM^+IgD^+ cells in the bone marrow. Thus, *Cd81*$^{-/-}$ mice provide an example where B cell are hyperactive although there is increased generation of IgM^+IgD^+ cells, which play a major role in T-independent B cell response.

Based on the results presented here, we conclude that one of the physiological roles of CD81 is to serve as a negative regulator of B cell activation. Most of the B cell-specific cell surface molecule known to inhibit B cell activation contains immunoreceptor tyrosine-based inhibition motifs (ITIMs). In general, B cells that lack molecules containing ITIM, including CD22, FcγRII and PIR-B, are hyperactivate in response to BCR stimulation but respond normally to LPS (54). Therefore, these molecules primarily modify BCR signaling. Since, CD81 lacks ITIM and our results show that CD81-deficient B cells are hyperactive in response to stimulation either via BCR or TLR4 and exhibit enhanced downstream signaling events (Figs 1–3 and supplementary Figure S2 is available at *International Immunology* Online), we hypothesize that CD81 may exert its effect at the cell membrane.

Supplementary data

Supplementary Figures S1–S4 and Table S1 are available at *International Immunology* Online.

(300 rad) *Rag1*$^{-/-}$ mice via the tail vein. (F) Spleen cells from the adoptive transfer recipients were stained with fluorochrome-conjugated anti-CD19 and CD3 antibodies and analyzed by flow cytometry. (G) B cell adoptive transfer *Rag1*$^{-/-}$ recipients were immunized intra-peritoneally with 50 μg TNP–LPS. Sera were collected at the indicated time points and TNP-specific anti-IgM response was measured by ELISA. Anti-TNP IgM response from three mice from each group are shown as mean ± SD. Significance of difference of mean values are indicated by asterisk (*$P \leqslant 0.05$, **$P \leqslant 0.001$ and ***$P \leqslant 0.0001$).

Funding

Leukemia and Lymphoma Society (7751).

Acknowledgements

We thank Ron Levy and Leonore Herzenberg for their continuous advice in this study and to Peter Wilker for sharing his expertise of B cell proliferation assay. The authors declare that they have no competing financial interests.

Abbreviations

BCR	B cell receptor
CFSE	carboxyfluorescein succinimidyl ester
Erk	extracellular signal-regulated kinase
ITIM	immunoreceptor tyrosine-based inhibition motif
NF-κB	nuclear factor-kappa B
PLCγ2	phospholipase gamma 2
SyK	spleen tyrosine kinase
TEM	tetraspanin-enriched microdomain
TLR	toll like receptor
TNP	2,4,6, trinitrophenol

References

1 Seigneuret, M. 2006. Complete predicted three-dimensional structure of the facilitator transmembrane protein and hepatitis C virus receptor CD81: conserved and variable structural domains in the tetraspanin superfamily. *Biophys. J.* 90:212.
2 Hemler, M. E. 2003. Tetraspanin proteins mediate cellular penetration, invasion, and fusion events and define a novel type of membrane microdomain. *Annu. Rev. Cell Dev. Biol.* 19:397.
3 Levy, S. and Shoham, T. 2005. The tetraspanin web modulates immune-signalling complexes. *Nat. Rev. Immunol.* 5:136.
4 Nydegger, S., Khurana, S., Krementsov, D. N., Foti, M. and Thali, M. 2006. Mapping of tetraspanin-enriched microdomains that can function as gateways for HIV-1. *J. Cell Biol.* 173:795.
5 Levy, S., Todd, S. C. and Maecker, H. T. 1998. CD81 (TAPA-1): a molecule involved in signal transduction and cell adhesion in the immune system. *Annu. Rev. Immunol.* 16:89.
6 Pileri, P., Uematsu, Y., Campagnoli, S. *et al.* 1998. Binding of hepatitis C virus to CD81. *Science* 282:938.
7 Silvie, O., Rubinstein, E., Franetich, J. F. *et al.* 2003. Hepatocyte CD81 is required for *Plasmodium falciparum* and *Plasmodium yoelii* sporozoite infectivity. *Nat. Med.* 9:93.
8 Bradbury, L. E., Kansas, G. S., Levy, S., Evans, R. L. and Tedder, T. F. 1992. The CD19/CD21 signal transducing complex of human B lymphocytes includes the target of antiproliferative antibody-1 and Leu-13 molecules. *J. Immunol.* 149:2841.
9 Matsumoto, A. K., Martin, D. R., Carter, R. H., Klickstein, L. B., Ahearn, J. M. and Fearon, D. T. 1993. Functional dissection of the CD21/CD19/TAPA-1/Leu-13 complex of B lymphocytes. *J. Exp. Med.* 178:1407.
10 Dempsey, P. W., Allison, M. E., Akkaraju, S., Goodnow, C. C. and Fearon, D. T. 1996. C3d of complement as a molecular adjuvant: bridging innate and acquired immunity. *Science* 271:348.
11 Carter, R. H. and Fearon, D. T. 1992. CD19: lowering the threshold for antigen receptor stimulation of B lymphocytes. *Science* 256:105.
12 Depoil, D., Fleire, S., Treanor, B. L. *et al.* 2008. CD19 is essential for B cell activation by promoting B cell receptor-antigen microcluster formation in response to membrane-bound ligand. *Nat. Immunol.* 9:63.
13 Rickert, R. C., Rajewsky, K. and Roes, J. 1995. Impairment of T-cell-dependent B-cell responses and B-1 cell development in CD19-deficient mice. *Nature* 376:352.
14 Sato, S., Miller, A. S., Howard, M. C. and Tedder, T. F. 1997. Regulation of B lymphocyte development and activation by the CD19/CD21/CD81/Leu 13 complex requires the cytoplasmic domain of CD19. *J. Immunol.* 159:3278.
15 Wang, Y., Brooks, S. R., Li, X., Anzelon, A. N., Rickert, R. C. and Carter, R. H. 2002. The physiologic role of CD19 cytoplasmic tyrosines. *Immunity* 17:501.
16 Maecker, H. T. and Levy, S. 1997. Normal lymphocyte development but delayed humoral immune response in CD81-null mice. *J. Exp. Med.* 185:1505.
17 Miyazaki, T., Muller, U. and Campbell, K. S. 1997. Normal development but differentially altered proliferative responses of lymphocytes in mice lacking CD81. *EMBO J.* 16:4217.
18 Tsitsikov, E. N., Gutierrez-Ramos, J. C. and Geha, R. S. 1997. Impaired CD19 expression and signaling, enhanced antibody response to type II T independent antigen and reduction of B-1 cells in CD81-deficient mice. *Proc. Natl Acad. Sci. USA* 94:10844.
19 van Zelm, M. C., Smet, J., Mascart, F. *et al.* 2008. Antibody-deficiency and acute nephritic syndrome in a patient with homozygous disruption of the CD81 gene. In: *ASH Annual Meeting Abstracts. Blood* 112:83.
20 Shoham, T., Rajapaksa, R., Boucheix, C. *et al.* 2003. The tetraspanin CD81 regulates the expression of CD19 during B cell development in a postendoplasmic reticulum compartment. *J. Immunol.* 171:4062.
21 Shoham, T., Rajapaksa, R., Kuo, C. C., Haimovich, J. and Levy, S. 2006. Building of the tetraspanin web: distinct structural domains of CD81 function in different cellular compartments. *Mol. Cell. Biol.* 26:1373.
22 Masciopinto, F., Freer, G., Burgio, V. L. *et al.* 2002. Expression of human CD81 in transgenic mice does not confer susceptibility to hepatitis C virus infection. *Virology* 304:187.
23 Sanyal, M., Tung, J. W., Karsunky, H. *et al.* 2007. B-cell development fails in the absence of the Pbx1 proto-oncogene. *Blood* 109:4191.
24 Krutzik, P. O., Clutter, M. R. and Nolan, G. P. 2005. Coordinate analysis of murine immune cell surface markers and intracellular phosphoproteins by flow cytometry. *J. Immunol.* 175:2357.
25 Di Virgilio, F., Steinberg, T. H. and Silverstein, S. C. 1990. Inhibition of Fura-2 sequestration and secretion with organic anion transport blockers. *Cell Calcium* 11:57.
26 Feske, S. 2007. Calcium signalling in lymphocyte activation and disease. *Nat. Rev. Immunol.* 7:690.
27 Scharenberg, A. M., Humphries, L. A. and Rawlings, D. J. 2007. Calcium signalling and cell-fate choice in B cells. *Nat. Rev. Immunol.* 7:778.
28 Andersson, J., Sjoberg, O. and Moller, G. 1972. Induction of immunoglobulin and antibody synthesis *in vitro* by lipopolysaccharides. *Eur. J. Immunol.* 2:349.
29 Miller, A. T., Sandberg, M., Huang, Y. H. *et al.* 2007. Production of Ins(1,3,4,5)P4 mediated by the kinase Itpkb inhibits store-operated calcium channels and regulates B cell selection and activation. *Nat. Immunol.* 8:514.
30 Parker, D. C. 1993. T cell-dependent B cell activation. *Annu. Rev. Immunol.* 11:331.
31 Cariappa, A., Chase, C., Liu, H., Russell, P. and Pillai, S. 2007. Naive recirculating B cells mature simultaneously in the spleen and bone marrow. *Blood* 109:2339.
32 Hardy, R. R., Carmack, C. E., Shinton, S. A., Kemp, J. D. and Hayakawa, K. 1991. Resolution and characterization of pro-B and pre-pro-B cell stages in normal mouse bone marrow. *J. Exp. Med.* 173:1213.
33 Cariappa, A., Mazo, I. B., Chase, C. *et al.* 2005. Perisinusoidal B cells in the bone marrow participate in T-independent responses to blood-borne microbes. *Immunity* 23:397.
34 Cherukuri, A., Shoham, T., Sohn, H. W. *et al.* 2004. The tetraspanin CD81 is necessary for partitioning of coligated CD19/CD21-B cell antigen receptor complexes into signaling-active lipid rafts. *J. Immunol.* 172:370.
35 Hardy, R. R. and Hayakawa, K. 2001. B cell development pathways. *Annu. Rev. Immunol.* 19:595.
36 Li, Y. S., Wasserman, R., Hayakawa, K. and Hardy, R. R. 1996. Identification of the earliest B lineage stage in mouse bone marrow. *Immunity* 5:527.
37 van Zelm, M. C., Reisli, I., van der Burg, M. *et al.* 2006. An antibody-deficiency syndrome due to mutations in the CD19 gene. *N. Engl. J. Med.* 354:1901.

38 Kanegane, H., Agematsu, K., Futatani, T. *et al.* 2007. Novel mutations in a Japanese patient with CD19 deficiency. *Genes Immun.* 8:663.
39 Engel, P., Zhou, L. J., Ord, D. C., Sato, S., Koller, B. and Tedder, T. F. 1995. Abnormal B lymphocyte development, activation, and differentiation in mice that lack or overexpress the CD19 signal transduction molecule. *Immunity* 3:39.
40 Fehr, T., Rickert, R. C., Odermatt, B. *et al.* 1998. Antiviral protection and germinal center formation, but impaired B cell memory in the absence of CD19. *J. Exp. Med.* 188:145.
41 Pezzutto, A., Dorken, B., Rabinovitch, P. S., Ledbetter, J. A., Moldenhauer, G. and Clark, E. A. 1987. CD19 monoclonal antibody HD37 inhibits anti-immunoglobulin-induced B cell activation and proliferation. *J. Immunol.* 138:2793.
42 Carter, R. H., Tuveson, D. A., Park, D. J., Rhee, S. G. and Fearon, D. T. 1991. The CD19 complex of B lymphocytes. Activation of phospholipase C by a protein tyrosine kinase-dependent pathway that can be enhanced by the membrane IgM complex. *J. Immunol.* 147:3663.
43 Fujimoto, M., Bradney, A. P., Poe, J. C., Steeber, D. A. and Tedder, T. F. 1999. Modulation of B lymphocyte antigen receptor signal transduction by a CD19/CD22 regulatory loop. *Immunity* 11:191.
44 Campbell, K. S. 1999. Signal transduction from the B cell antigen-receptor. *Curr. Opin. Immunol.* 11:256.
45 Deng, J., Dekruyff, R. H., Freeman, G. J., Umetsu, D. T. and Levy, S. 2002. Critical role of CD81 in cognate T-B cell interactions leading to Th2 responses. *Int. Immunol.* 14:513.
46 Maecker, H. T., Do, M. S. and Levy, S. 1998. CD81 on B cells promotes interleukin 4 secretion and antibody production during T helper type 2 immune responses. *Proc. Natl Acad. Sci. USA* 95:2458.
47 Boismenu, R., Rhein, M., Fischer, W. H. and Havran, W. L. 1996. A role for CD81 in early T cell development. *Science* 271:198.
48 Conley, M. E., Rohrer, J., Rapalus, L., Boylin, E. C. and Minegishi, Y. 2000. Defects in early B-cell development: comparing the consequences of abnormalities in pre-BCR signaling in the human and the mouse. *Immunol. Rev.* 178:75.
49 Wang, J. H., Avitahl, N., Cariappa, A. *et al.* 1998. Aiolos regulates B cell activation and maturation to effector state. *Immunity* 9:543.
50 O'Keefe, T. L., Williams, G. T., Davies, S. L. and Neuberger, M. S. 1996. Hyperresponsive B cells in CD22-deficient mice. *Science* 274:798.
51 Otipoby, K. L., Andersson, K. B., Draves, K. E. *et al.* 1996. CD22 regulates thymus-independent responses and the lifespan of B cells. *Nature* 384:634.
52 Sato, S., Miller, A. S., Inaoki, M. *et al.* 1996. CD22 is both a positive and negative regulator of B lymphocyte antigen receptor signal transduction: altered signaling in CD22-deficient mice. *Immunity* 5:551.
53 Pan, C., Baumgarth, N. and Parnes, J. R. 1999. CD72-deficient mice reveal nonredundant roles of CD72 in B cell development and activation. *Immunity* 11:495.
54 Xu, Y., Harder, K. W., Huntington, N. D., Hibbs, M. L. and Tarlinton, D. M. 2005. Lyn tyrosine kinase: accentuating the positive and the negative. *Immunity* 22:9.
55 Tung, J. W., Parks, D. R., Moore, W. A., Herzenberg, L. A. and Herzenberg, L. A. 2004. Identification of B-cell subsets: an exposition of 11-color (Hi-D) FACS methods. *Methods Mol. Biol.* 271:37.

Spplemental Figures and Table

Enhanced B cell activation in the absence of CD81

Mrinmoy Sanyal, Rosemary Fernandez and Shoshana Levy

International Immunology, Vol. 21, No. 11, pp. 1225–1237
doi:10.1093/intimm/dxp090

Content

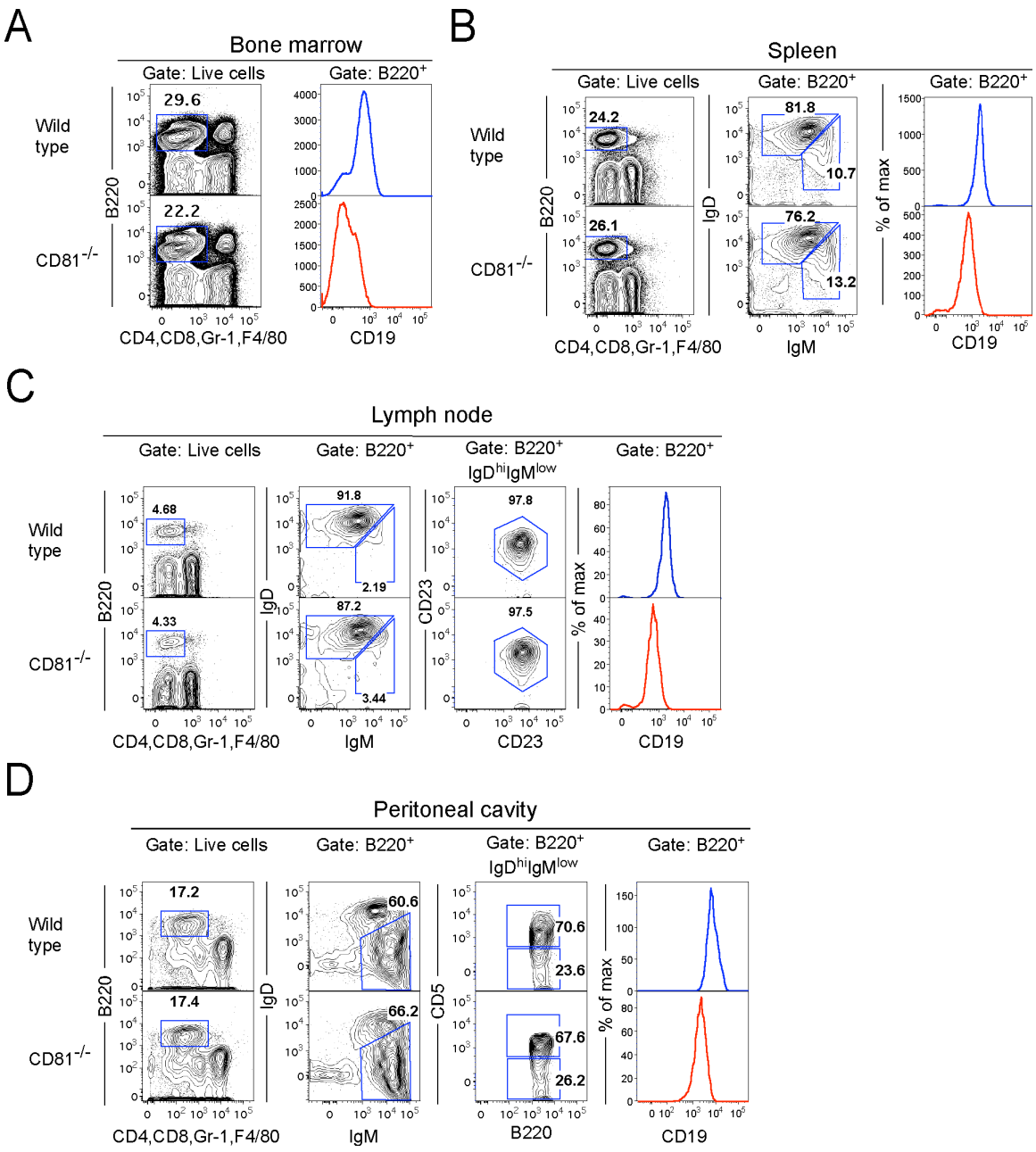

Supplemental Figure S1. Reduced CD19 expression in *Cd81*$^{-/-}$ B cells.

A. Bone marrow cells were stained with fluorochrome conjugated anti- B220, anti-CD4, CD8, Gr-1, F4/80, and anti-CD19 antibodies and analyzed by flow cytometry. Plotted is CD19 expression in gated B220^{+} wild type (blue) and *Cd81*$^{-/-}$ (red) cells.

B. Spleen cells were stained with fluorochrome conjugated anti- B220, anti-CD4, CD8, Gr-1, F4/80, anti-IgM, anti-IgD, and anti-CD19 antibodies. CD19 expression in gated B220^{+} cells is shown as in A.

C. B cell subsets in lymph node and **D**. peritoneal cavity of *Cd81*$^{-/-}$ and wild type mice. Cells were stained with fluorochrome conjugated anti- B220, anti-CD4, CD8, Gr-1, F4/80, anti-IgM, anti-IgD, and anti-CD5 antibodies and analyzed by flow cytometry. CD19 expression in gated B220^{+} cells is shown as in A.

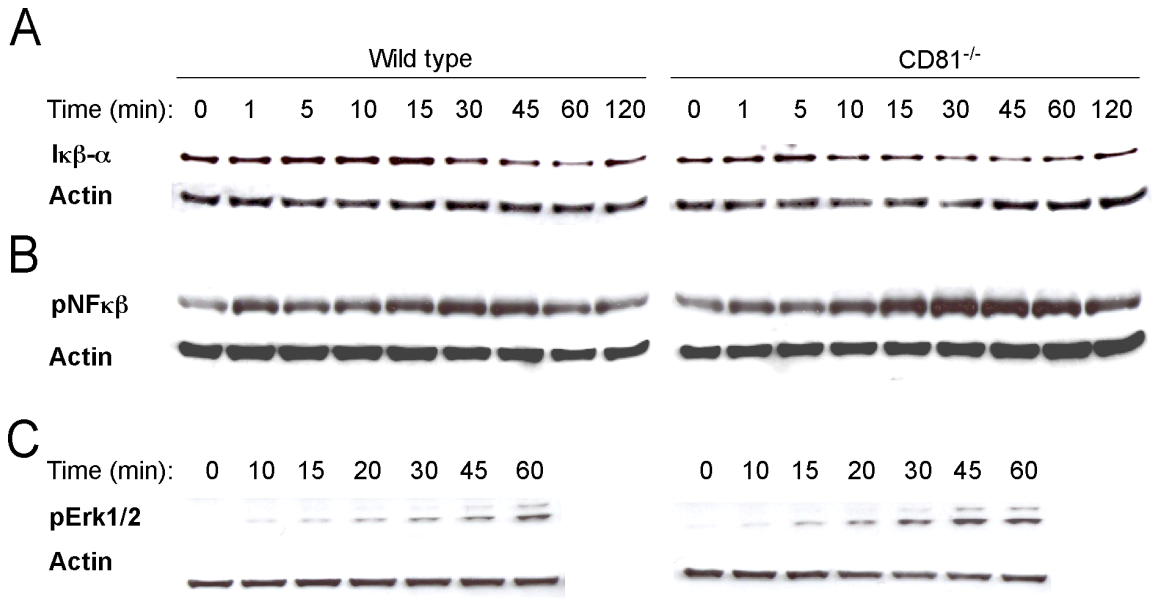

Supplemental Figure S2. LPS-induced intracellular signaling is enhanced in *Cd81*$^{-/-}$ B cells.

Purified B cells were stimulated for indicated times with 10 μg/ml LPS and subjected to western blot analysis. The blots were striped and re-probed with anti-actin antibody. **A.** Degradation of Iκβ–α in wild type and *Cd81*$^{-/-}$ B cells, note an earlier degradation in CD81-defficient B cells. **B.** Phosphorylation of NFκβ in wild type and *Cd81*$^{-/-}$ B cells. CD81-defficient B cells showed a moderately increased phosphorylation of NFκβ. **C.** Phosphorylation of ERK1/2 in wild type and *Cd81*$^{-/-}$ B cells, note earlier phosphorylation in ERK1/2 in CD81-defficient B cells. The figure is representative of three independent experiments.

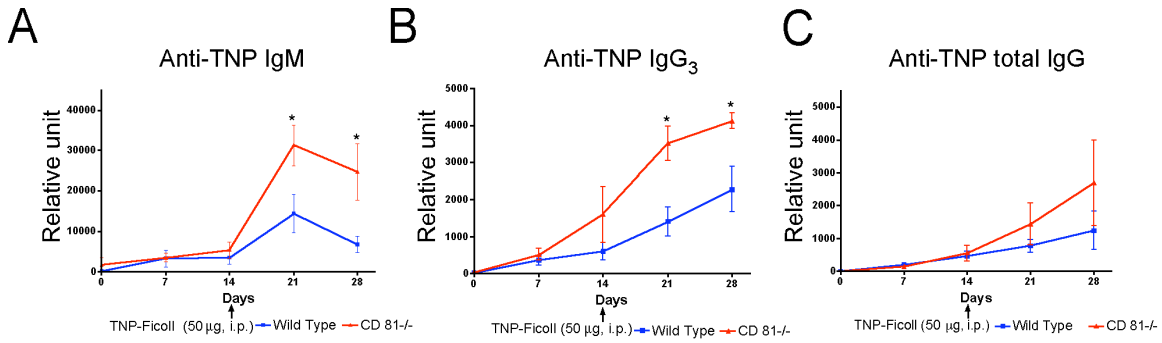

Supplemental Figure S3. Increased immune response to the T-independent antigen TNP-ficoll in *Cd81*$^{-/-}$ mice.

Wild type and *Cd81*$^{-/-}$ mice (N=3 each) were immunized intra-peritoneally with TNP-ficoll (50 µg/ml) and boosted 2 weeks after the initial immunization. Pre-immune and post-immune sera were collected and TNP-specific IgM (**A**), IgG_3 (**B**) and total IgG (**C**) was measured by ELISA. Plotted is the response of wild type (blue) and *Cd81*$^{-/-}$ (red) mice as mean ± SD. Significance of difference of mean values are indicated by stars (* $p \leq 0.05$, ** $p \leq 0.001$ and *** $p \leq 0.0001$).

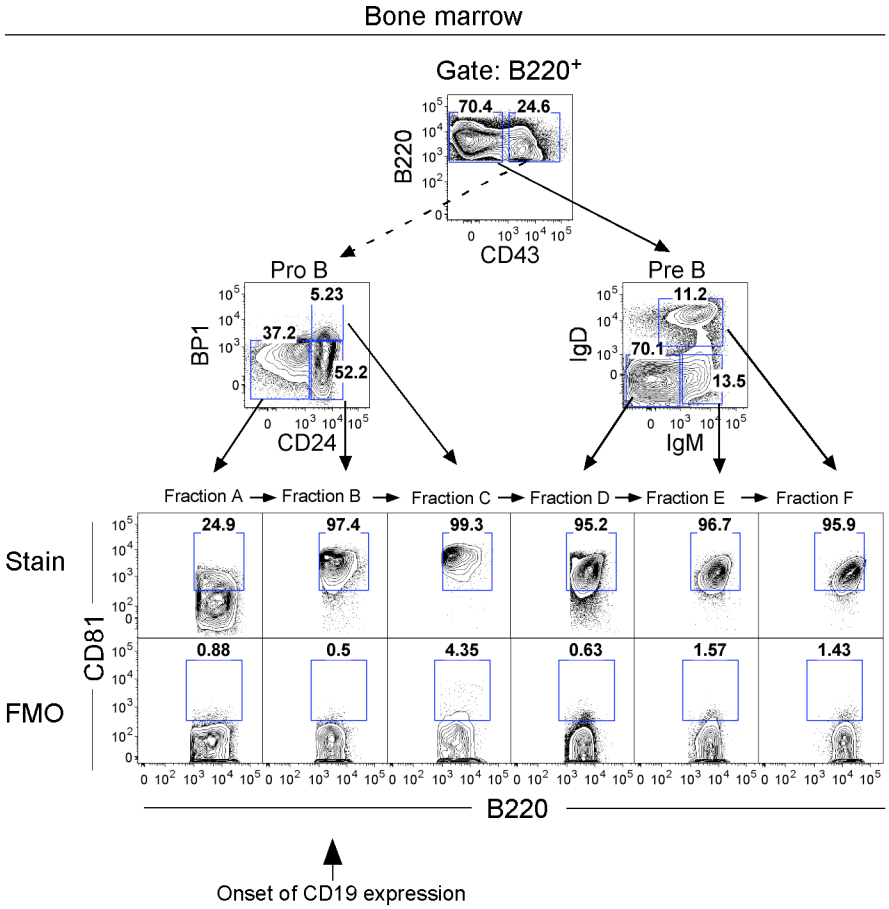

Supplemental Figure S4. Expression of CD81 during B cell development.

Bone marrow cells from a normal Balb/c mouse were stained with fluorochrome conjugated anti-mouse B220, CD43, BP-1, CD24, IgM, IgD and CD81 monoclonal antibodies (1,2) to resolve the B cell developmental stages. $B220^{+}CD43^{+}$ and $B220^{+}CD43^{-}$ cells were further resolved (fractions A-F). Finally, CD81 expression was determined in these fractions. Background fluorescent intensity was determined by a separate stain with combination of antibodies excluding anti-CD81 antibody (Fluorescence minus one; FMO) and shown below the respective fraction.

A continued high level of CD81 expression was observed in all stages of B cell development except the earliest stage corresponding fraction A where a very low level of expression was observed. Note that the expression of both CD19 and CD81 start at fraction B, the pro-B cells stage of B cell development (3).

References

1 Hardy, R. R., Carmack, C. E., Shinton, S. A., Kemp, J. D., and Hayakawa, K. 1991. Resolution and characterization of pro-B and pre-pro-B cell stages in normal mouse bone marrow. *J Exp Med* 173:1213-25.

2 Tung, J. W., Parks, D. R., Moore, W. A., Herzenberg, L. A., and Herzenberg, L. A. 2004. Identification of B-cell subsets: an exposition of 11-color (Hi-D) FACS methods. *Methods Mol Biol* 271:37-58.

3 Li, Y. S., Wasserman, R., Hayakawa, K., and Hardy, R. R. 1996. Identification of the earliest B lineage stage in mouse bone marrow. *Immunity* 5:527-35.

Table S1 (Supplemental). Antibodies used for flow cytometric analysis

Antigen	Clone	Conjugation	Application
B220	RA3-6B2	APC,Cy5PE, PerCP-Cy5.5	B cells, Hardy profile, Phosphoflow
CD19	1D3	Fluorescein, Biotin	B cells
CD24	30-F1	Biotin	Hardy profile
CD43	S7	PE	B cells, Hardy profile
CD81	Eat-2	PE, Biotin	Expression analysis
BP-1	6C31BP1	Alexa594	Hardy profile
IgM (Igh-6a)	DS-1	PE	Mature B cells
IgM	331	APC-Cy7	Mature B cells, Hardy profile
IgD	11-26	PE-Cy7	Mature B cells, Hardy profile
CD5	53-7.3	PE-Cy5	B1 B cells
CD21	7G6	Fluorescein	Mature B cells
CD23	B3-B4	Alexa 594	Mature B cells
TCRβ	H57-597	APC	T cells
NK1.1	PK136	PE	NK cells, Lineage
CD3	145-2C11	Cascade Blue, Alexa 488	Lineage, Phosphoflow
CD4	GK1.5	APC-Cy7, Cascade Blue	T cells
CD8	53-6.7	PE-Cy7, Cascade Blue	T cells
Gr1	RB6-8C5	Cascade Blue	Lineage
CD11b	Mac-1	Cascade Blue	Lineage
Pan-macrophage	F4/80	Cascade Blue	Lineage
Ki67	B56	Fluorescein	Cell proliferation
CD80	16-10A1	Fluorescein	Activation marker
CD86	GL1	PE	Activation marker
CD69	H1.2F3	PE-Cy7	Activation marker
Phospho-Syk (pY351)	17A/P-ZAP70	Alexa Fluor- 647	Phosphoflow
Phospho-PLCγ2 (pY759)	K86-689.37	Alexa Fluor- 488	Phosphoflow